ACS **APPLIED** MATERIALS & INTERFACES

# Regulating Aggregated Structures in Organohydrogels for On-Demand Information Encryption

Fuqing Shan, Xiaoxia Le,* Hui Shang, Weiping Xie, Wei Sun,* and Tao Chen*

Cite This: *ACS Appl. Mater. Interfaces* 2023, 15, 7405−7413

Read Online

ACCESS | Metrics & More | Article Recommendations | Supporting Information

**ABSTRACT:** As one of the most promising candidates for dynamic information storage, intelligent gels with tunable optical properties under external stimuli have received great attention. The implementation of transparency variation for information display is a favorable and versatile strategy but still faces the challenge of on-demand encryption–decryption. Herein, an optical tunable organohydrogel is prepared, which has interpenetrating heterogeneous networks consisting of hydrophilic poly(N,N-dimethylacrylamide) (PDMA) and hydrophobic polyoctadecyl methacrylate (PSMA). The long alkane side chains of PSMA endow the organohydrogel with the capacity of crystallization–melting transitions under the stimulus of heat, accompanied by transparent–opaque switching. In addition, the variations of transparency can also be achieved by water-induced hydrophobic association and microphase separation, resulting from the unique heterogeneous networks of the organohydrogel. Based on the abovementioned two aggregated structures, various pieces of information can be loaded on the organohydrogel by light writing or water printing with the assistance of masks. The coded information can be encrypted and decrypted by solvent replacement and temperature switching. This elaborately designed organohydrogel can act as an effective communication platform with an improved security level and ignite the sparks of developing novel information storage materials.

**KEYWORDS:** *aggregated structures, organohydrogel, stimulus responsiveness, information encryption, information decryption*
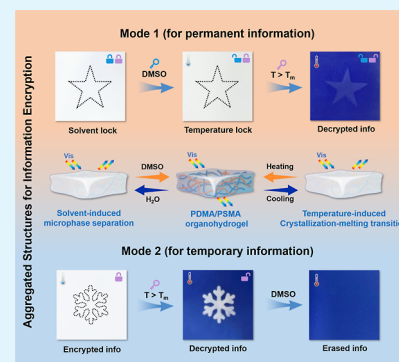
## 1. INTRODUCTION

Natural organisms provide numerous vivid demonstrations for the design of smart artificial materials that possess sophisticated structures and astonishing functions. Considering a typical example, cephalopods (*e.g.*, cuttlefish, squid, and octopus) can change their apparent transparency or colors by adjusting the aggregated morphology of pigment cells to adapt to their surroundings for camouflage, communication, attraction, and so forth.[1−4] Inspired by these intriguing phenomena, a plenty of artificial materials that are able to change their optical properties have been fabricated, which have been utilized for camouflage skins,[5−8] smart windows,[9−13] and information displays.[14−17]

As one of the most promising artificial materials with discoloration behavior, smart gels can change their optical properties (*e.g.*, fluorescence, structural color, and transparency) in response to external stimuli such as heat, light, magnetism, electricity, and so on.[18−20] Due to the programmable structures and unique stimulus responsiveness, a series of optical switchable materials based on smart gels have been fabricated.[21−24] For example, Tang *et al.* proposed a multifluorescent supramolecular hydrogel formed by interfacial supramolecular adhesion between four hydrogel units that contain different aggregation-induced emission dots and demonstrated its capability to store large amounts of information using a "codes in code" method.[25] Zhao *et al.*

demonstrated a self-healing structural color hydrogel by using healable protein hydrogel-filled inverse opal scaffolds, which can be further assembled and healed to construct one-dimensional linear microfibers, two-dimensional patterns, and three-dimensional photonic pathway structures.[26] However, these systems rely on the synthesis of pigment molecules or construction of micro–nano structures, which either is dependent on certain illumination or limited to suitable templates.

To fabricate gels with tunable optical properties, implementation of transparency variation seems to be favorable and versatile. A common strategy to endow smart gels with remarkable capabilities to change transparency is by way of establishing aggregated structures, including crystallization, microphase separation, inorganic additives, and self-assembling.[27] For instance, inspired by the memorizing–forgetting behavior of human brain, Gong *et al.* designed a soft hydrogel that enables rapid water uptake and slow water release, which can exhibit transparency change under the stimulus of heat due
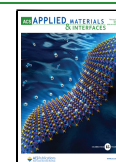
**Scheme 1. Schematic Illustration of Optical Tunable PDMA/PSMA Organohydrogels; (a) As-prepared Organohydrogel Composed of the Hydrophilic Monomer DMA-Based Hydrogel Network and Hydrophobic Monomer SMA-Based Organogel Network; (b) Schematic Mechanism of the Organohydrogel in Transparency Variations, Which Are Triggered by Solvent Displacement or Temperature Change; (c) Two Encryption−Decryption Modes for Permanent Information and Temporary Information, Respectively**
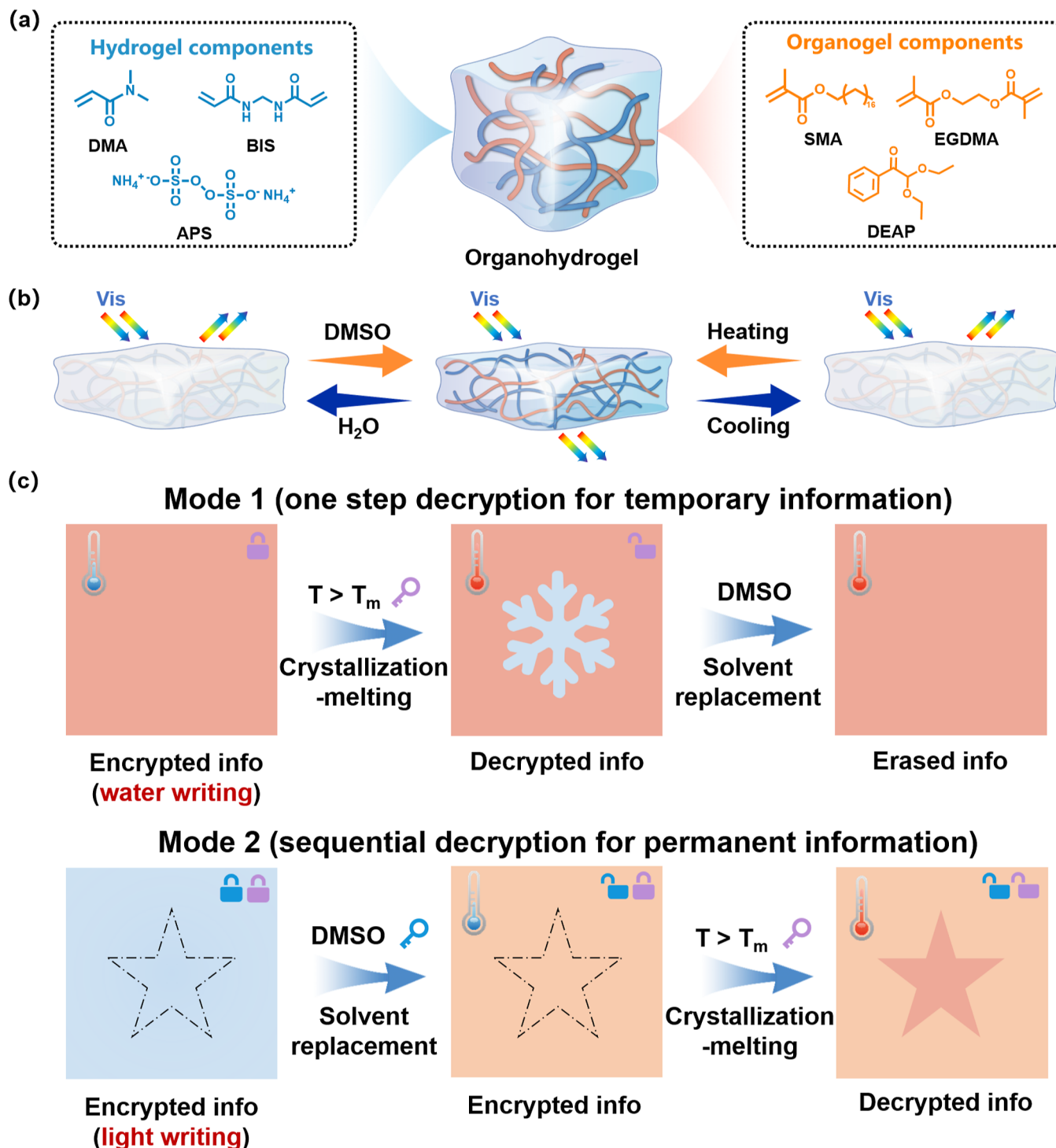


to the internal thermal-sensitive dynamic bonds.[28] Chen *et al.* reported an organohydrogel that shows apparent transparent−opaque variation in response to poor solvents generated from microphase separation, which can act as a dynamic information-recognition platform.[29] These elegant efforts have been made to achieve information display based on transparency change but are still limited by the lack of on-

demand encryption−decryption behavior, which improve the level of information security.

Herein, a well-designed organohydrogel with interpenetrating networks was fabricated, which consists of the hydrophilic poly(*N,N*-dimethylacrylamide) (PDMA) network and hydrophobic polyoctadecyl methacrylate (PSMA) network bearing long crystalline alkyl chains (Scheme 1a). Taking advantage of
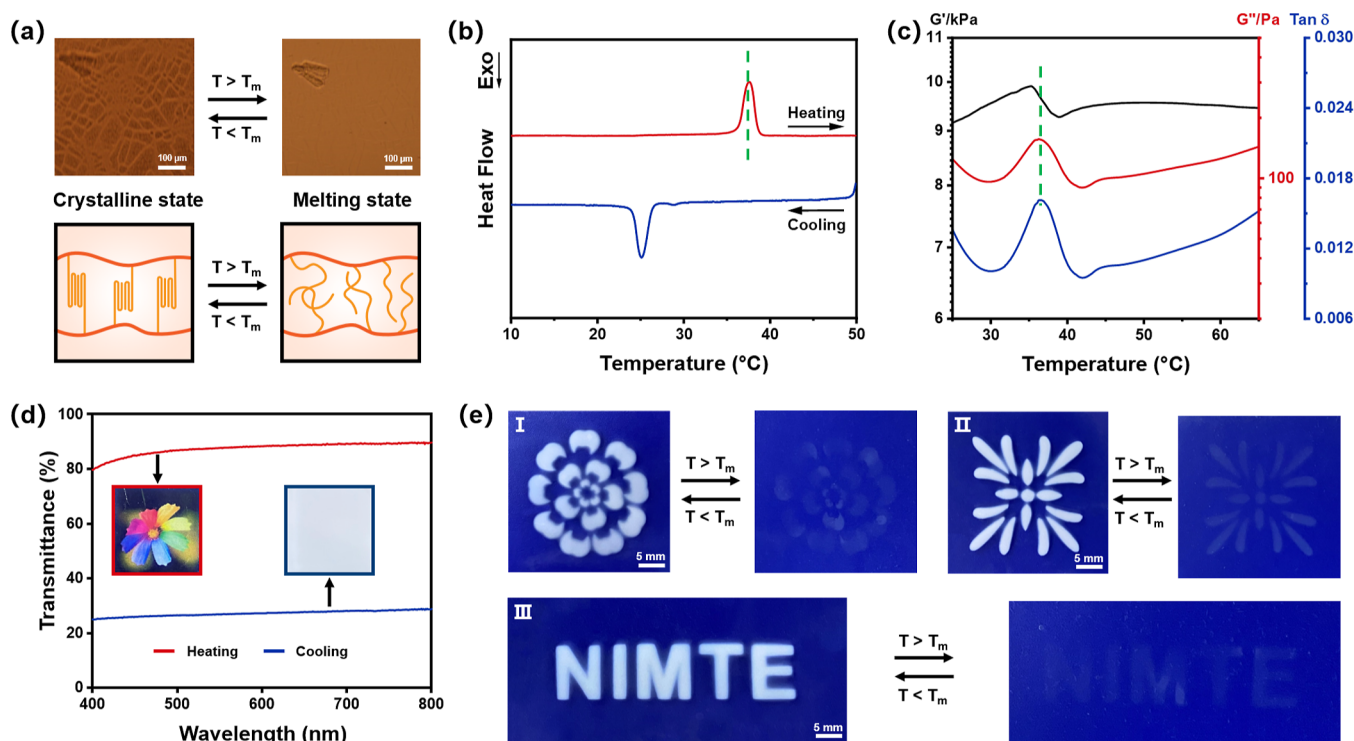
**Figure 1.** Tunable optical behavior of the PDMA/PSMA organohydrogel based on crystallization−melting phase transition. (a) Polarizing microscopy images and schematic diagram of the PDMA/PSMA organohydrogel at crystallization and melting states. (b) DSC crystallization and melting curves. (c) Temperature sweep data of the PDMA/PSMA organohydrogel at a constant shear strain of 1% and a frequency of 10 rad·s$^{-1}$. (d) Transmittance and photographs of the PDMA/PSMA organohydrogel at crystallization and melting states. (e) Different optical patterns (*e.g.*, flowers and letters) obtained with the assistance of photomasks, which display and disappear through the temperature switches. The scale bar is 5 mm.

the heterogeneous networks, aggregated structures of both the crystallization phase and solvent-induced hydrophobic microphase were innovatively obtained in one organohydrogel system. The crystallization−melting transition caused by alkyl chains can be triggered by applying the thermal stimulus, and the water-induced microphase separation can be terminated when the solvent was replaced by dimethyl sulfoxide (DMSO). As the abovementioned two processes were accompanied by opaque−transparent transformation (Scheme 1b), the organohydrogel can serve as an information display platform with the assistance of suitable masks for both temporary information (mode 1) and permanent information (mode 2). Specifically, the temporary information (snowflake) written by water can be decrypted by applying a thermal stimulus, which can further be erased by immersing in DMSO solution in mode 1. As for mode 2, light-written permanent information (such as five-pointed star) can only be decrypted by controlling the sequence of solvent replacement and temperature increase (Scheme 1c). This organohydrogel-based information display platform may provide a novel strategy for designing information anti-counterfeiting materials and broadening the promising application fields of smart gels.

## 2. EXPERIMENTAL SECTION

**2.1. Materials.** *N,N*-Dimethylacrylamide (DMA), ammonium persulfate (APS), *N,N′*-methylene bis(acrylamide) (MBA), *N,N,N′,N′*-tetramethylethylenediamine (TEMED), 2,2-diethoxyace-tophenone (DEAP), and ethylene dimethacrylate (EGDMA) were commercially provided by Aladdin Reagent Co., Ltd. Stearyl methacrylate (SMA) was purchased from J&K Scientific Ltd. All reagents were used without any treatment or purification.

**2.2. Preparation of the PDMA Hydrogel.** The PDMA hydrogel was synthesized by free-radical polymerization. DMA (5 g), APS (50 mg), MBA (5 mg), and TEMED (50 μL) were added into 10 mL of deionized water. After being completely mixed, the solution was rapidly injected into a homemade mold and then placed at ambient temperature for 24 h for gelation. Finally, the resultant hydrogel was put into acetone for dehydration and removing unreacted monomers.
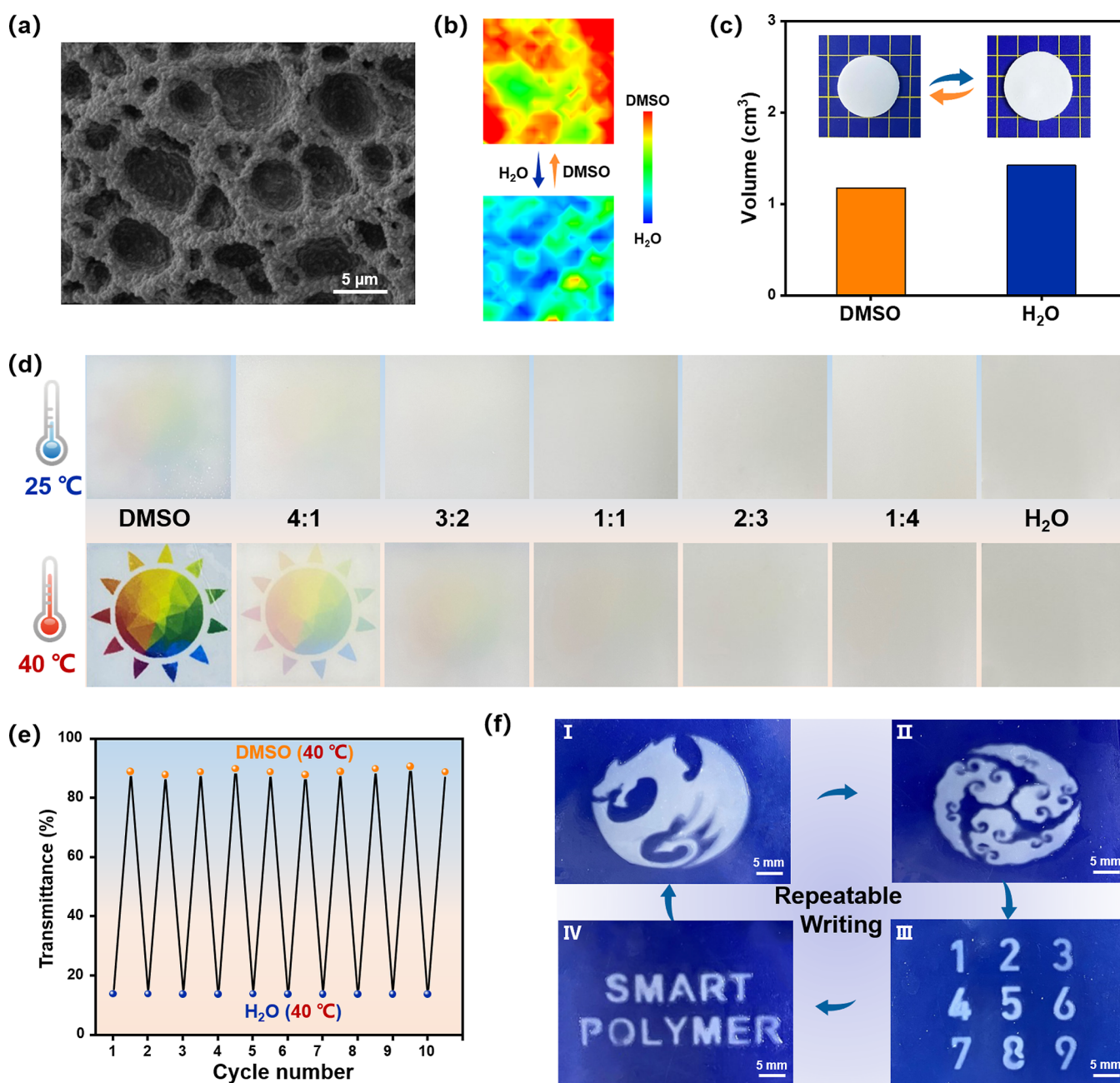
**2.3. Preparation of the PDMA/PSMA Organohydrogel.** First, SMA (50 g), DEAP (500 mg), and EGDMA (50 mg) were dissolved in 100 g of ethanol. The dehydrated hydrogel was subsequently soaked into the prepared solution and kept in the dark for 12 h. Finally, the PDMA/PSMA organohydrogel was obtained by exposing the mixture to 365 nm UV light and then submerged into DMSO to remove unreacted monomers.

**2.4. SEM Characterization.** The samples were first treated with water for solvent replacement and then immersed in liquid nitrogen to preserve the microstructures. Next, the samples were lyophilized in a freeze-dryer (ODENG, LCJ-10D, China) for 24 h. The cross-sectional morphology of the organohydrogel was characterized by field-emission scanning electron microscopy (SEM, S-4800, Hitachi).

**2.5. Transmittance Testing.** A UV−vis spectrophotometer (TU-1810, Purkinje General Instrument Co., Ltd.) was used to characterize the light transmittance of the gel in the wavelength range from 400 to 800 nm.

**2.6. ATR-FTIR Characterization.** Fourier transform infrared spectra were obtained through an attenuated total reflection Fourier transformed infrared spectrometer (ATR-FTIR, Thermo Scientific Nicolet 6700).

**2.7. CA Measurements.** The contact angles (CAs) were measured with a DO3210 machine at ambient temperature. The volume of the droplet dropped on the gel surface was precisely controlled at 3 μL.

**Figure 2.** PDMA/PSMA organohydrogel for information display based on water-induced microphase separation. (a) Cross-sectional SEM image of the PDMA/PSMA organohydrogel. The scale bar is 5 $\mu$m. (b) 2D scan images of Fourier infrared spectra when the heteronetwork was filled with DMSO and $H_2O$. (c) Photographs and volumes of a wafer-shaped organohydrogel after reaching the swelling equilibrium in DMSO and $H_2O$. (d) Photographs of PDMA/PSMA organohydrogels swollen by different ratios of DMSO to water at 25 and 40 °C. (e) Cyclic changes in transparency during solvent replacement at a temperature of 40 °C. (f) Photographs of rewritable information (*e.g.*, patterns, numbers, and letters), in which the white areas were emerged by water treatment. The scale bar is 5 mm.

**2.8. Rheological Tests.** The rheological characterizations were performed on a rheometer (TA, DHR-3) equipped with a 25 mm parallel plate.

**2.9. Raman Characterization.** Raman spectra were obtained by using a Raman spectrometer (Renishaw inVia Reflex) using a green light-emitting diode laser (532 nm).

## 3. RESULTS AND DISCUSSION

**3.1. Preparation and Characterization of the Heteronetwork Organohydrogel.** In this study, a two-step free radical polymerization method was utilized to prepare an organohydrogel with heterogeneous networks (Figure S1,

Supporting Information).[30,31] Briefly, the hydrophilic PDMA hydrogel was first constructed *via* thermal polymerization in the presence of MBA as a cross-linker and APS as an initiator. After dehydration in acetone, the xerogel was submerged and swelled until equilibrium in ethanol solution, which contains the hydrophobic crystalline monomer SMA, ethyl dimethacrylate (EGDMA) as a cross-linker, and DEAP as a photoinitiator. Subsequently, the hydrogel network filled with oily precursor solution was exposed to UV light for obtaining an organohydrogel with interpenetrating networks *in situ*. Finally, the unreacted monomers were removed when the solvent was replaced by DMSO.

As the successful introduction of the organogel network was essential for this system, the chemical composition of the PDMA/PSMA organohydrogel was first investigated. In order to confirm the successful introduction of the organogel network, ATR-FTIR was employed (Figure S2, Supporting Information). Compared to the PDMA hydrogel, the organohydrogel shows a characteristic peak at 1727.9 cm$^{-1}$, which corresponds to the stretching vibrations of C=O in the ester group of SMA. In addition, the organohydrogel possesses characteristic peaks at 2915.8 and 2848.3 cm$^{-1}$, which are attributed to the stretching vibrations of the C−H bond associated to alkyl chains of SMA.[32] In addition, the differences between the PDMA hydrogel and PDMA/PSMA organohydrogel could also be distinguished by rheological behavior. As shown in Figure S2b, the storage modulus ($G'$) and loss modulus ($G''$) of the PDMA/PSMA organohydrogel were both higher than that of the PDMA hydrogel with a certain frequency range (0.1 to 100 rad·s$^{-1}$ at a strain of 1%), indicating that the introduction of the interpenetrating network can obviously enhance the mechanical properties of the original hydrogel network. Furthermore, the PDMA/PSMA organohydrogel with an interpenetrating heterogeneous network possesses a higher CA of 94.7° than that of the PDMA hydrogel, demonstrating the successful formation of the heteronetwork organohydrogel (Figure S3, Supporting Information).

### 3.2. Tunable Optical Behavior of the Organohydrogel Based on Crystallization−Melting Phase Transition.

The presence of long alkyl chains in hydrophobic PSMA network confers crystallization behavior onto the as-prepared organohydrogel. The polarized optical microscopy images directly showed that the crystalline microregions disappeared with the increase in temperature, which reappeared when the temperature went down (Figure 1a). In addition, the differential scanning calorimetry (DSC) curve in Figure 1b demonstrated a sharp peak at around 38 °C, which can be ascribed to the crystallization−melting phase transition of PSMA.[33,34] A similar phase transition temperature in accordance with DSC data could also be observed through rheological testing. As illustrated in Figure 1c, the storage modulus ($G'$) exhibited a step-like decrease, and the loss modulus ($G''$) and damping factor (tan $\delta$) show obvious peaks at about 38 °C during the temperature sweep process. Due to the crystallization−melting transition, the optical properties of the organohydrogel are greatly affected. As shown in the plots of transmittance (Figure 1d), the PDMA/PSMA organohydrogel exhibited obvious optical variation, totally transparent (more than 80%) at 40 °C and completely opaque (less than 30%) at 25 °C. Furthermore, Raman spectroscopy was conducted to monitor peak shifts during crystallization and melting. When the prepared sample was heated from 25 to 55 °C, significant shifting of characteristic peaks could be seen (Figure S4, Supporting Information).

Given that the PDMA/PSMA organohydrogel undergoes conspicuous transparent−opaque transition, information display and hiding can be achieved under the stimulation of temperature. As the PSMA network was introduced into the PDMA network by *in situ* photopolymerization, varying patterns can be obtained by light writing with the help of photomasks (Figure S5, Supporting Information). As depicted in Figure 1e, patterns such as "Sakura", "Chrysanthemum", and "NIMTE" can be permanently recorded during the process of preparing organohydrogels by utilizing corresponding masks.

When the temperature was higher than $T_m$, all the patterns basically disappeared due to the crystallization−melting transition, which would show up again if the temperature drops back. What is more, it is worth noting that the spatial resolution of our lithographic patterns is about 200 $\mu$m (Figure S6, Supporting Information), close to the limit of resolution ratio of human eyes.

### 3.3. Tunable Optical Behavior of Organohydrogels Based on Microphase Separation.

Owing to the unique heterogeneous network structure, the well-designed organohydrogel possesses tunable optical behavior under the stimulation of solvents. The microstructure of the organohydrogel was first observed by scanning electron microscopy (SEM). As illustrated in Figure 2a, the hydrophobic PSMA network was uniformly attached to the hydrophilic PDMA network in the form of spheres, resulting from the microphase separation and hydrophobic association in water. The long alkyl chains of PSMA have a propensity to form hydrophobic microdomains when the heterogeneous networks are saturated with water. As a polar organic solvent, DMSO is not only soluble with water but also miscible with most organics; thus, it was chosen for solvent replacement (Figure S7, Supporting Information). Taking a piece of PDMA/PSMA organohydrogel for example, an obvious color change can be observed on two-dimensional Fourier infrared mappings, indicating a rapid solvent exchange between DMSO and H$_2$O (Figure 2b).

As shown in Figure 2c, the organohydrogel was opaque when equilibrated either in water or in DMSO at room temperature, accompanied by slight volume change due to mutual constrain between the hydrophilic network and hydrophobic network. Although apparent properties were not affected, the internal structure of the organohydrogel has changed significantly. When the solvent is DMSO, the PSMA chains could undergo crystallization−melting phase transition or even migration at high temperature, thus increasing the transparency of the organohydrogel. If the solvent is water, hydrophobic PSMA chains collapsed, associated, and formed microdomains, which cannot be destructed by direct heating. As a result, the transparency of the organohydrogel gradually decreased as the proportion of water increased, originating from the formation of hydrophobic microdomains that prevented the transmission of light (Figures 2d and S8, Supporting Information). What is more, only when the solvent of pure DMSO was used, can opaque−transparent transition occur. In other words, the dominance of the aggregated structure in this organohydrogel system depends on the choices of solvents, DMSO for crystalline regions and H$_2$O for hydrophobic microdomains.

In order to assess the durability and stability of the organohydrogel, repetitive transparent−opaque switching was conducted. As shown in Figure 2e, the organohydrogel sample exhibited inconspicuous variation in transmittance even after 10 cycles of solvent replacement, showing promising potential for application of repeatable writing. For proving the concept, a PET mask with well-designed hollow patterns was attached onto the surface of an organohydrogel, and water was cast onto the hollowed-out regions for information writing. As shown in Figure 2f, a series of patterns, including "dragon", "auspicious cloud", numbers "123456789", and letters "SMART POLYMER", were acquired by sequential writing by H$_2$O and erasing by DMSO (Figure S9, Supporting Information). The resolution of the water-writing patterns was approximately
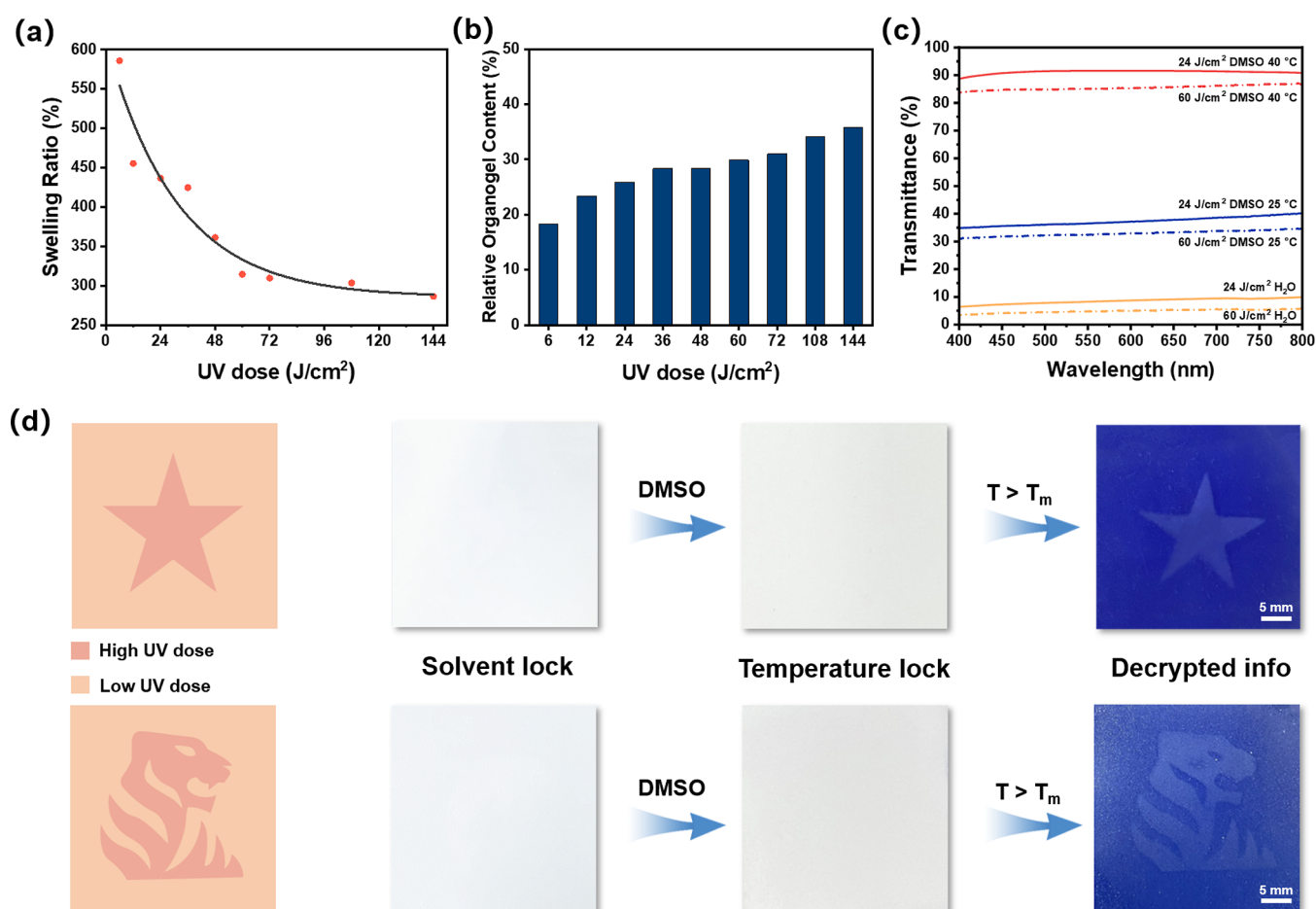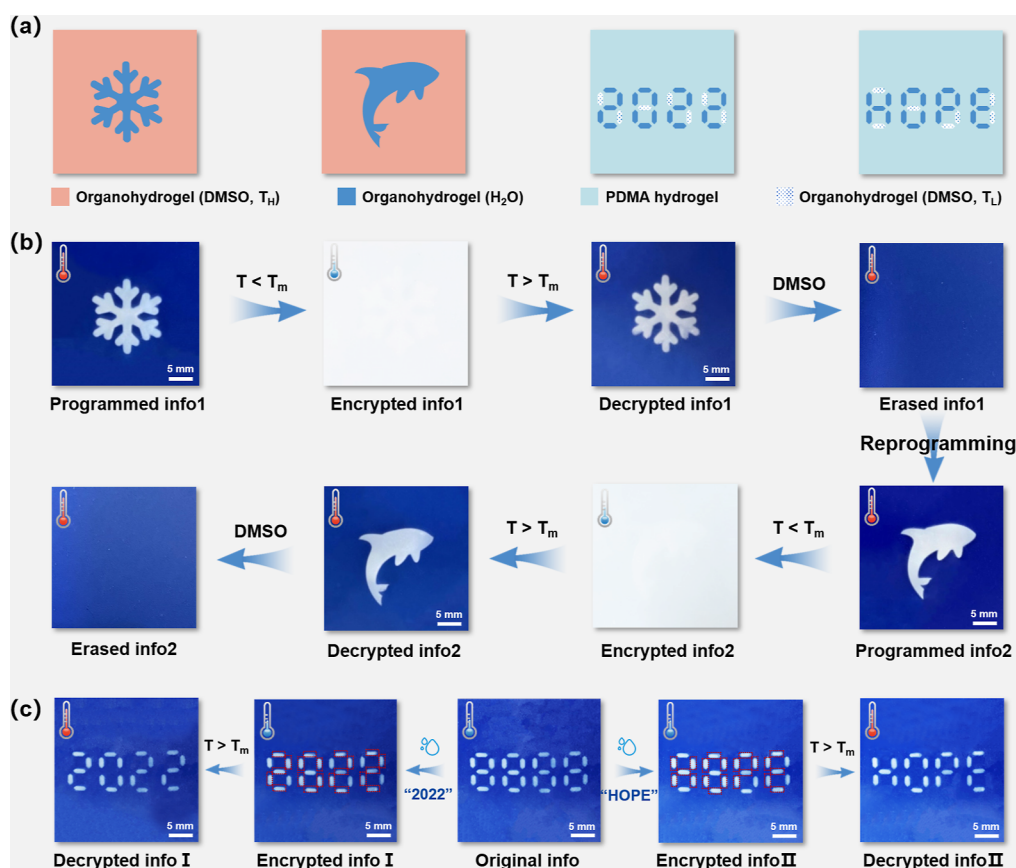
**Figure 3.** Information encryption−decryption achieved by controlling cross-linking domains of the PDMA/PSMA organohydrogel. (a) Swelling ratio of the PDMA/PSMA organohydrogel as a function of the UV dose. (b) Proportion of the organogel network as a function of the UV dose. (c) Transmittance of PDMA/PSMA organohydrogels that were prepared with a high UV dose (60 J/cm$^2$) and low UV dose (24 J/cm$^2$) at 25 and 40 °C, respectively. (d) Secret patterns obtained by local exposure to different UV doses that enable dual encryption−decryption. The scale bar is 5 mm.

300 $\mu$m (Figure S10, Supporting Information), which ensures the accuracy of complicated information writing.

**3.4. Dual-Responsive Organohydrogel for Information Encryption and Decryption.** With two aggregated structures coexisting in the organohydrogel, information encryption and decryption can be achieved by employing appropriate stimulation step by step. Two different encryption−decryption modes have been revealed based on this organohydrogel system: (1) target information generated by light writing is permanent, and subsequent information encryption and decryption were achieved through solvent replacement and temperature switching in sequence. (2) Using water as ink, target information written down on the PDMA/PSMA organohydrogel is temporary, and temperature variation is the only way to achieve information encryption−decryption. What is more, the target information can be erased by solvent replacement, leading to new information loading on the organohydrogel.

For the first encryption−decryption mode, the energy density of UV irradiation becomes the key factor to realize information encryption−decryption. Irradiation time and illumination intensity could be used to adjust covalent cross-linking density, thus producing spatio-temporally grayscale images.[35] Taking both irradiation time and light intensity into consideration, the UV dose was used in our system (Formula

S1, Supporting Information). As can be seen in Figure 3a, the swelling ratio of the fabricated organohydrogels decreased with the increase in UV dose, which indicates the increase in organogel network and cross-linking density. In the meanwhile, the relative content of the organogel network was measured by the weighting method. The result indicates that more and more PSMA network was introduced into the PDMA gel network with the increase in UV dose (Figure 3b). As illustrated in Figure 3c, organohydrogels obtained with UV doses of 24 and 60 J/cm$^2$ show neglectable differences in transmittance when the solvent is H$_2$O or DMSO at low temperature (25 °C), which can be utilized for hiding images. Only when the temperature increases, the transparency of organohydrogels that were swollen by DMSO increased dramatically, and the contrast of organohydrogels with different UV doses would be enhanced. Based on the difference in transmittance, a novel double-lock system can be designed for dual-information encryption and decryption. As shown in Figure 3d, the desired regions (deep orange, *e.g.*, star and tiger) were obtained by exposure to a higher irradiation dose of UV light than that of the background region (light orange), causing the difference of the gray scale for information coding. The elaborate patterns were locked by solvent (H$_2$O) and temperature (25 °C), which were accessible when the solvent was replaced by DMSO and the

**Figure 4.** Dual-responsive PDMA/PSMA organohydrogel for information encryption. (a) Schematic diagram of gels that are encoded with various pieces of information *via* mask-assisted local patterning. Orange represents the PDMA/PSMA organohydrogel filled with DMSO at high temperature (40 °C). Blue represents the PDMA/PSMA organohydrogel swollen by water. Cyan stands for the PDMA hydrogel. White parts are the PDMA/PSMA organohydrogel with DMSO at low temperature (25 °C). (b) Various patterns loaded by mask-assisted water treatment. The patterns can be hided/reappeared by temperature switching and erased by solvent displacement. (c) Encryption−decryption processes of numbers "2022" and letters "HOPE".

temperature increased to 40 °C in sequence. It should be noted that the "unlocking" order is important. Only when the solvent replacement is implemented first, can the information show up, which notably improves the information security.

Another encryption−decryption mode is achieved by water printing of desired patterns on the PDMA/PSMA organohydrogel. Original regions swollen by DMSO are capable of crystallization−melting phase transition, while the patterned regions swollen by water would have no transition due to water-induced microphase separation. Consequently, the encrypted information can emerge when the temperature is above $T_m$, originated from the melting crystalline regions and unchanged hydrophobic microdomains. As depicted in Figure 4a, a series of patterns such as snowflake, dolphin, the numbers "2022", and the letters "HOPE" were designed according to the abovementioned ideas. In detail, the orange area represents the portion of the organohydrogel that is swollen by DMSO at 40 °C, the blue part is the portion of the organohydrogel that is treated with water, the cyan region identifies the portion of the PDMA hydrogel that shows no responsiveness to any stimulus, and the white part is the portion of the organohydrogel that is swollen by DMSO at 25 °C.

As a proof-of-concept, the programmed "snowflake" pattern was loaded on the organohydrogel (DMSO, 40 °C) with the assistance of a customized mask, followed by cooling to room temperature (25 °C) for information hiding. When the

information needs to be read, we should just increase the temperature above melting temperature, making the crystalline region become transparent and keeping the hydrophobic microdomains constant. What is more, the loaded information on the organohydrogel can be wiped by replacing the solvent with DMSO, which can act as a new platform that can be used again. Therefore, a new programmed pattern "dolphin" can be printed, hided, displayed, and erased, indicating remarkable reversibility of the organohydrogel.

Generally, it is rather challenging to distinguish real information from the false one, especially when they are similar. Information camouflage can be achieved when a false information can be transformed to the real one under certain conditions, providing information security. By using the versatile light writing technique, the PDMA/PSMA organohydrogel can be endowed with various patterns, on which the real information can be loaded *via* the water-writing process. As a result, the information displayed under normal circumstances is fake, and the true one only emerges when exposed to the stimulus of heat. For instance, a fake information "8888" written *via* light writing consisted of the DMSO-swollen PDMA/PSMA organohydrogel, which could undergo opaque−transparent transition under temperature stimulation. Information such as "2022" or "HOPE" was written by water based on "8888" but exhibited no difference between them. Only when the temperature went up, can the encrypted

information be visible due to the hydrophobic regions without thermal responsiveness (Figure 4c).

## 4. CONCLUSIONS

In summary, an organohydrogel containing stimulus-responsive aggregated structures has been designed for on-demand information encryption−decryption. The interpenetrating networks consist of a hydrophilic PDMA network and a hydrophobic PSMA network, exhibiting thermal-regulated crystallization−melting transition and opaque−transparent transformation. In addition, the heterogeneous networks endow the organohydrogel with solvent-controlled hydrophobic microphase separation, which was also accompanied by changes in transparency. When the solvent of DMSO was used, the organohydrogel responded to temperature switching with the variation of transparency. Once integrated with water, hydrophobic microdomains were produced so that the organohydrogel lost the capacity of transparent−opaque transition. Taking advantage of the different stimulus responsiveness of two aggregated structures, programmed patterns with similar opacity can be obtained by using suitable masks, leading to the encryption and decryption of either permanent or temporary information under the stimuli of solvent and temperature. The establishment of the organohydrogel in the current study exhibits great potential as an information display platform. It also provides a new route for developing information anti-counterfeiting materials and enriching encryption−decryption techniques.

## ■ ASSOCIATED CONTENT

### ⓢ Supporting Information

The Supporting Information is available free of charge at https://pubs.acs.org/doi/10.1021/acsami.2c21020.

> Schematic of the preparation process of the organohydrogel; FTIR spectra and rheological properties of the PDMA hydrogel and PDMA/PSMA organohydrogel; CAs of the PDMA hydrogel and PDMA/PSMA organohydrogel; Raman spectrum of the PDMA/PSMA organohydrogel at 25 and 55 °C, respectively; spatial resolution evaluation of light writing and water writing; schematic illustration of light writing, solvent replacement and water writing; transmittance variations of PDMA/PSMA organohydrogels with varying ratios of solvents at 25 and 40 °C, respectively; and calculation equation of the UV radiation dose (PDF)

## ■ AUTHOR INFORMATION

### Corresponding Authors

**Xiaoxia Le** − *Key Laboratory of Marine Materials and Related Technologies, Zhejiang Key Laboratory of Marine Materials and Protective Technologies, Ningbo Institute of Material Technology and Engineering, Chinese Academy of Sciences, Ningbo 315201, China; School of Chemical Sciences, University of Chinese Academy of Sciences, Beijing 100049, China;* ⓞ orcid.org/0000-0003-3716-3076; Email: lexiaoxia@nimte.ac.cn

**Wei Sun** − *School of Materials Science and Chemical Engineering, Ningbo University, Ningbo 315211, China;* ⓞ orcid.org/0000-0002-2923-5554; Email: sunwei@nbu.edu.cn

**Tao Chen** − *Key Laboratory of Marine Materials and Related Technologies, Zhejiang Key Laboratory of Marine Materials and Protective Technologies, Ningbo Institute of Material Technology and Engineering, Chinese Academy of Sciences, Ningbo 315201, China; School of Chemical Sciences, University of Chinese Academy of Sciences, Beijing 100049, China;* ⓞ orcid.org/0000-0001-9704-9545; Email: tao.chen@nimte.ac.cn

### Authors

**Fuqing Shan** − *School of Materials Science and Chemical Engineering, Ningbo University, Ningbo 315211, China; Key Laboratory of Marine Materials and Related Technologies, Zhejiang Key Laboratory of Marine Materials and Protective Technologies, Ningbo Institute of Material Technology and Engineering, Chinese Academy of Sciences, Ningbo 315201, China*

**Hui Shang** − *Key Laboratory of Marine Materials and Related Technologies, Zhejiang Key Laboratory of Marine Materials and Protective Technologies, Ningbo Institute of Material Technology and Engineering, Chinese Academy of Sciences, Ningbo 315201, China; School of Chemical Sciences, University of Chinese Academy of Sciences, Beijing 100049, China*

**Weiping Xie** − *Public Technology Center, Ningbo Institute of Material Technology and Engineering, Chinese Academy of Sciences, Ningbo 315201, China*

Complete contact information is available at:
https://pubs.acs.org/10.1021/acsami.2c21020

### Notes

The authors declare no competing financial interest.

## ■ ACKNOWLEDGMENTS

## ■ REFERENCES

(1) Mäthger, L. M.; Senft, S. L.; Gao, M.; Karaveli, S.; Bell, G. R. R.; Zia, R.; Kuzirian, A. M.; Dennis, P. B.; Crookes-Goodson, W. J.; Naik, R. R.; Kattawar, G. W.; Hanlon, R. T. Bright White Scattering from Protein Spheres in Color Changing, Flexible Cuttlefish Skin. *Adv. Funct. Mater.* **2013**, *23*, 3980−3989.

(2) Kreit, E.; Mäthger, L. M.; Hanlon, R. T.; Dennis, P. B.; Naik, R. R.; Forsythe, E.; Heikenfeld, J. Biological Versus Electronic Adaptive Coloration: How Can One Inform The Other? *J. R. Soc., Interface* **2013**, *10*, 20120601.

(3) Mäthger, L. M.; Denton, E. J.; Marshall, N. J.; Hanlon, R. T. Mechanisms and Behavioural Functions of Structural Coloration in Cephalopods. *J. R. Soc., Interface* **2009**, *6*, S149−S163.

(4) Hanlon, R. Cephalopod Dynamic Camouflage. *Curr. Biol.* **2007**, *17*, R400−R404.

(5) Wei, S.; Qiu, H.; Shi, H.; Lu, W.; Liu, H.; Yan, H.; Zhang, D.; Zhang, J.; Theato, P.; Wei, Y.; Chen, T. Promotion of Color-Changing Luminescent Hydrogels from Thermo to Electrical Responsiveness toward Biomimetic Skin Applications. *ACS Nano* **2021**, *15*, 10415−10427.

(6) Won, P.; Kim, K. K.; Kim, H.; Park, J. J.; Ha, I.; Shin, J.; Jung, J.; Cho, H.; Kwon, J.; Lee, H.; Ko, S. H. Transparent Soft Actuators/Sensors and Camouflage Skins for Imperceptible Soft Robotics. *Adv. Mater.* **2021**, *33*, 2002397.

(7) Pikul, J. H.; Li, S.; Bai, H.; Hanlon, R. T.; Cohen, I.; Shepherd, R. F. Stretchable Surfaces with Programmable 3D Texture Morphing for Synthetic Camouflaging Skins. *Science* **2017**, *358*, 210−214.

(8) Kang, W.; Lin, M.-F.; Chen, J.; Lee, P. S. Highly Transparent Conducting Nanopaper for Solid State Foldable Electrochromic Devices. *Small* **2016**, *12*, 6370−6377.

(9) Li, J.; Lu, X.; Zhang, Y.; Ke, X.; Wen, X.; Cheng, F.; Wei, C.; Li, Y.; Yao, K.; Yang, S. Highly Sensitive Mechanoresponsive Smart Windows Driven by Shear Strain. *Adv. Funct. Mater.* **2021**, *31*, 2102350.

(10) Guo, M.; Yu, Q.; Wang, X.; Xu, W.; Wei, Y.; Ma, Y.; Yu, J.; Ding, B. Tailoring Broad-Band-Absorbed Thermoplasmonic 1D Nanochains for Smart Windows with Adaptive Solar Modulation. *ACS Appl. Mater. Interfaces* **2021**, *13*, 5634−5644.

(11) Chen, C.; Huang, Z.; Zhu, S.; Liu, B.; Li, J.; Hu, Y.; Wu, D.; Chu, J. In Situ Electric-Induced Switchable Transparency and Wettability on Laser-Ablated Bioinspired Paraffin-Impregnated Slippery Surfaces. *Adv. Sci.* **2021**, *8*, 2100701.

(12) Zhang, Q.; Jiang, Y.; Chen, L.; Chen, W.; Li, J.; Cai, Y.; Ma, C.; Xu, W.; Lu, Y.; Jia, X.; Bao, Z. Ultra-Compliant and Tough Thermochromic Polymer for Self-Regulated Smart Windows. *Adv. Funct. Mater.* **2021**, *31*, 2100686.

(13) Lin, C.; Hur, J.; Chao, C. Y. H.; Liu, G.; Yao, S.; Li, W.; Huang, B. All-Weather Thermochromic Windows for Synchronous Solar and Thermal Radiation Regulation. *Sci. Adv.* **2022**, *8*, No. eabn7359.

(14) Deng, S.; Huang, L.; Wu, J.; Pan, P.; Zhao, Q.; Xie, T. Bioinspired Dual-Mode Temporal Communication via Digitally Programmable Phase-Change Materials. *Adv. Mater.* **2021**, *33*, 2008119.

(15) Oh, H.; Lee, J. K.; Kim, Y. M.; Yun, T. Y.; Jeong, U.; Moon, H. C. User-Customized, Multicolor, Transparent Electrochemical Displays Based on Oxidatively Tuned Electrochromic Ion Gels. *ACS Appl. Mater. Interfaces* **2019**, *11*, 45959−45968.

(16) Kim, J.-W.; Myoung, J.-M. Flexible and Transparent Electrochromic Displays with Simultaneously Implementable Subpixelated Ion Gel-Based Viologens by Multiple Patterning. *Adv. Funct. Mater.* **2019**, *29*, 1808911.

(17) Yang, J.; Lim, T.; Jeong, S. M.; Ju, S. Information-Providing Flexible and Transparent Smart Window Display. *ACS Appl. Mater. Interfaces* **2021**, *13*, 20689−20697.

(18) Lou, D.; Sun, Y.; Li, J.; Zheng, Y.; Zhou, Z.; Yang, J.; Pan, C.; Zheng, Z.; Chen, X.; Liu, W. Double Lock Label Based on Thermosensitive Polymer Hydrogels for Information Camouflage and Multilevel Encryption. *Angew. Chem., Int. Ed.* **2022**, *61*, No. e202117066.

(19) Chen, X.; Han, G.; Ren, P.; Lyu, Q.; Li, M.; Zhang, L.; Zhu, J. Shape Memory Photonic Gels Enable Reversible Regulation of Photoluminescence: Towards Multiple Anti-Counterfeiting. *Chem. Eng. J.* **2022**, *446*, 136879.

(20) Zhang, H.; Li, Q.; Yang, Y.; Ji, X.; Sessler, J. L. Unlocking Chemically Encrypted Information Using Three Types of External Stimuli. *J. Am. Chem. Soc.* **2021**, *143*, 18635−18642.

(21) Liu, J.; Guo, Q.; Zhang, X.; Gai, J.; Zhang, C. Multistage Responsive Materials for Real-time, Reversible, and Sustainable Light-Writing. *Adv. Funct. Mater.* **2021**, *31*, 2106673.

(22) Shang, H.; Le, X.; Si, M.; Wu, S.; Peng, Y.; Shan, F.; Wu, S.; Chen, T. Biomimetic Organohydrogel Actuator with High Response Speed and Synergistic Fluorescent Variation. *Chem. Eng. J.* **2022**, *429*, 132290.

(23) Zhu, C. N.; Bai, T.; Wang, H.; Ling, J.; Huang, F.; Hong, W.; Zheng, Q.; Wu, Z. L. Dual-Encryption in a Shape-Memory Hydrogel with Tunable Fluorescence and Reconfigurable Architecture. *Adv. Mater.* **2021**, *33*, 2102023.

(24) Sun, Y.; Le, X.; Zhou, S.; Chen, T. Recent Progress in Smart Polymeric Gel-Based Information Storage for Anti-Counterfeiting. *Adv. Mater.* **2022**, *34*, 2201262.

(25) Yang, Y.; Li, Q.; Zhang, H.; Liu, H.; Ji, X.; Tang, B. Z. Codes in Code: AIE Supramolecular Adhesive Hydrogels Store Huge Amounts of Information. *Adv. Mater.* **2021**, *33*, 2105418.

(26) Fu, F.; Chen, Z.; Zhao, Z.; Wang, H.; Shang, L.; Gu, Z.; Zhao, Y. Bio-Inspired Self-healing Structural Color Hydrogel. *Proc. Natl. Acad. Sci. U.S.A.* **2017**, *114*, 5900−5905.

(27) Cui, K.; Gong, J. P. Aggregated Structures and Their Functionalities in Hydrogels. *Aggregate* **2021**, *2*, No. e33.

(28) Yu, C.; Guo, H.; Cui, K.; Li, X.; Ye, Y. N.; Kurokawa, T.; Gong, J. P. Hydrogels as Dynamic Memory with Forgetting Ability. *Proc. Natl. Acad. Sci. U.S.A.* **2020**, *117*, 18962−18968.

(29) Chen, Z.; Chen, Y.; Guo, Y.; Yang, Z.; Li, H.; Liu, H. Paper-Structure Inspired Multiresponsive Hydrogels with Solvent-Induced Reversible Information Recording, Self-Encryption, and Multi-decryption. *Adv. Funct. Mater.* **2022**, *32*, 2201009.

(30) Gao, H.; Zhao, Z.; Cai, Y.; Zhou, J.; Hua, W.; Chen, L.; Wang, L.; Zhang, J.; Han, D.; Liu, M.; Jiang, L. Adaptive and Freeze-Tolerant Heteronetwork Organohydrogels with Enhanced Mechanical Stability over A Wide Temperature Range. *Nat. Commun.* **2017**, *8*, 15911.

(31) Zhuo, S.; Zhao, Z.; Xie, Z.; Hao, Y.; Xu, Y.; Zhao, T.; Li, H.; Knubben, E. M.; Wen, L.; Jiang, L.; Liu, M. Complex Multiphase Organohydrogels with Programmable Mechanics toward Adaptive Soft-matter Machines. *Sci. Adv.* **2020**, *6*, No. eaax1464.

(32) Le, X.; Shang, H.; Wu, S.; Zhang, J.; Liu, M.; Zheng, Y.; Chen, T. Heterogeneous Fluorescent Organohydrogel Enables Dynamic Anti-Counterfeiting. *Adv. Funct. Mater.* **2021**, *31*, 2108365.

(33) Bilici, C.; Okay, O. Shape Memory Hydrogels via Micellar Copolymerization of Acrylic Acid and n-Octadecyl Acrylate in Aqueous Media. *Macromolecules* **2013**, *46*, 3125−3131.

(34) Matsuda, A.; Sato, J. i.; Yasunaga, H.; Osada, Y. Order-Disorder Transition of a Hydrogel Containing an n-Alkyl Acrylate. *Macromolecules* **1994**, *27*, 7695−7698.

(35) Jiang, P.; Yan, C.; Ji, Z.; Guo, Y.; Zhang, X.; Jia, X.; Wang, X.; Zhou, F. Drawing High-Definition and Reversible Hydrogel Paintings with Grayscale Exposure. *ACS Appl. Mater. Interfaces* **2019**, *11*, 42586−42593.